

PAPER • OPEN ACCESS

## Dynamic Simulation of Gear System Based on 2D Space Multibody Physics: A Sustainable Gear Design Approach

To cite this article: E. Y. Salawu *et al* 2021 *IOP Conf. Ser.: Mater. Sci. Eng.* **1107** 012195

View the [article online](#) for updates and enhancements.

You may also like

- [Efficient analytical method to obtain the responses of a gear model with stochastic load and stochastic friction](#)  
Yining Fang, Ming J Zuo and Yue Li
- [Research on tooth profile modification of two spur gear driven system](#)  
Zhang Bin
- [Impact vibration response attenuation using four-bar linkage landing gear system](#)  
L Son and S Huda



The Electrochemical Society  
Advancing solid state & electrochemical science & technology

### 241st ECS Meeting

May 29 – June 2, 2022 Vancouver • BC • Canada

Abstract submission deadline: Dec 3, 2021

Connect. Engage. Champion. Empower. Accelerate.  
**We move science forward**



**Submit your abstract**



# Dynamic Simulation of Gear System Based on 2D Space Multibody Physics: A Sustainable Gear Design Approach

E.Y. Salawu<sup>1\*</sup>, O. O. Ajayi<sup>1</sup>, A. O. Inegbenebor<sup>1</sup>, Stephen Akinlabi<sup>1&2</sup>, S. A. Afolalu<sup>1</sup>,

B. M. Edun<sup>3</sup>

<sup>1</sup>Department of Mechanical Engineering, Covenant University, P.M.B. 1023, Ota, Ogun State, Nigeria

<sup>2</sup>Department of Mechanical Engineering, Walter Sisulu University, South Africa

<sup>3</sup>Department of Mechanical Engineering, Ogun State Institute of Technology, Igbesa

Corresponding Author: [enesi.salawu@covenantuniversity.edu.ng](mailto:enesi.salawu@covenantuniversity.edu.ng)

## Abstract

The study employed a two-dimensional (2D) space with multibody dynamics as the physics to simulate the dynamic behaviour of intermeshing gears. Both the gear teeth and the gear body were employed to simulate the principal stress and strain as well as the Von Mises stress of the gear system. A pair of meshing teeth were examined from the pinion and the other from the gear for accurate contact stress-strain simulation. The validity of the proposed gear simulation was verified from principal surface stress, Von Mises stress, principal surface strain, elastic strain and total displacement. The results show that the dynamic behaviour of the gear could be attributed to the critical meshing characteristics of the single and double teeth. The peak-to-peak pattern of the Von Mises stress indicates the essential points of stress, which could cause the occurrence of the failure modes. The research of the gear motion study is profoundly enriched and served as a critical reference for gear design.

**Keyword:** Gear, Design, Production, Sustainability, Simulation

## 1. Introduction

Spur gears have played an enormous role of power transmission in the field of equipment/machinery, and their dynamic behaviour owing to variation in the tooth geometry has a significant impact on the transmission performance and the overall reliability of the equipment [1]. Thus, one reason why an integrated approach must be adopted for modelling and predicting the likely occurrence of bending stress at the root of the tooth [2]. This failure occurring at the root region of the tooth was attributed to load distribution, improper operating conditions as well as flaws during the manufacturing of the gear. Thus, crack initiation occurs at the surface contact of the tooth, and this propagates into the material and causing complete fracture [3-5]. According to Pleguezuelos et al. [6], a quasi-static transmission error occurs in a pair of gears in mesh, which is attributed to load distribution at the teeth. This could result in excessive deflection of the gears and subsequent failure due to fatigue [7]. Although, several studies have recommended precision gear manufacturing approach to avert these incessant failures. For instance, Zhou et al. [8] proposed a point by point approach for grinding the tooth surface of a spur gear by introducing a conical spur shaper to achieve a precision finished gear. However, the grinding process was simulated to validate the actual manufacturing process of the gear. It was established that micro-pitting occurrence at the surface contact results into spalling and macro-pitting failures. Hence, it usually causes catastrophic damage to the entire gear system, which eventually tricky and costly to replace [9-13]. Gear tooth wear may be unavoidable, according to Zhiying and Pengfei [14] due to the load distribution between the tooth. However, an established relationship between the wear and load prediction will improve gear life. For instance,



Ouyang et al. [15] noted that a numerical approach (Runge-Kutta) for predicting the contact tribo-dynamic behaviour of spur gear system would improve the design and reliability of the system. More so, studies confirmed that bearing failure and backlash in gears could be attributed to chaotic motion in a rotating gear, which could lead to severe tooth damage [16]. Černe et al. [17] reported that such chaotic problem in a rotating spur gear creates system imbalance which could result in a high-temperature rise in the gear. Also, variation in the meshing stiffness and transmission error ensues which could increase vibration and subsequent damage [18-20]. Despite the developed models which have been used extensively in the prediction of load distribution on gear tooth, the simulation approach has been less exploited in stress-strain as well as displacement predictions [21]. More so, the variation in the meshing stiffness is usually calculated numerically, and details for predictions are limited [22-25]. Therefore, the severity of gear tooth failure could be reduced via simulation approach [26-30]. However, the majority of literature study paid less attention to the effect of tooth surface reaction such as stress, strain and tooth displacement. They focused on the geometry and the kinematic behaviour of a pair of gear in a mesh. Thus, the main focus of this study is to examine the possible behaviour of a pair of a spur gear in motion due to surface reaction force. To this end, a two dimensional (2D) representation of the gear was created using Comsol 2D space dimension with multibody dynamics as the physics attached to the simulation. This made it possible to simulate the instantaneous stress and strain experienced by the gear system. Thus, the study will inform gear designers of the importance of simulating the surface reaction forces, which will reduce continuous gear failure.

## 2. Simulation Procedure

The study employed the Comsol 5.3 version with multibody dynamics as the physics attached to the simulation, and a stationary study was done. Comsol 5.3 version was selected for this study due to its improved performance compared to the earlier version. It has the ability for solving, meshing, and the physics-based add-on makes it efficient to create models easily. Thus, the 2D representation of the gear was modelled using the 2D space dimension attached to the multibody dynamics, as shown in Figure 1. The number of teeth is 24, the pitch diameter is 0.05 m and a pressure angle of 20°, while the material used is cast iron.

## 3. Results and Discussion

Figure 1. present the 2D space dimension of the spur gear in a mesh. It indicates the motion study of a pair of spur gear in the mesh as well as the displacements in X and Y direction. The values displayed at the horizontal and vertical indicates the displacement of the gears in both directions. Thus, making it easy to understand the various stress analysis arising from the contact between the gears. Figure 2 presents the result of the surface principal stress on the gear tooth. It can be depicted from the result that the gear tooth experienced a multiaxial state of stress since the behaviour of the gear geometry reflects that of the principal stress state. More so, the surface principal stress was minimal at the line of action and the contact surface of the mating gears with a value of  $-4 \times 10^9 \text{ N/m}^2$ . However, the contact stress increased exponentially at the root fillet with a stress value of about  $8 \times 10^9 \text{ N/m}^2$ . This could initiate cracks and eventual wear of the teeth due to fatigue [31].

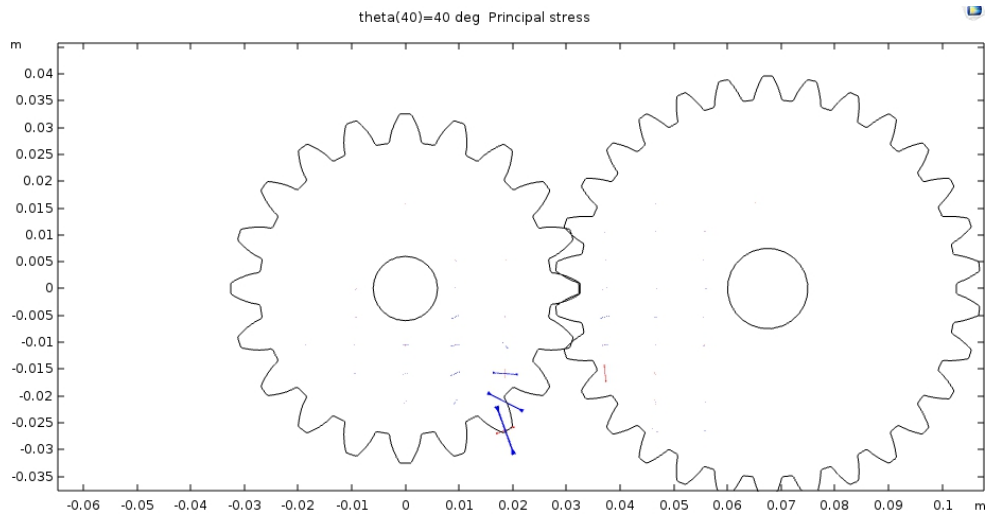


Fig 1: 2D space representation of the spur gear model

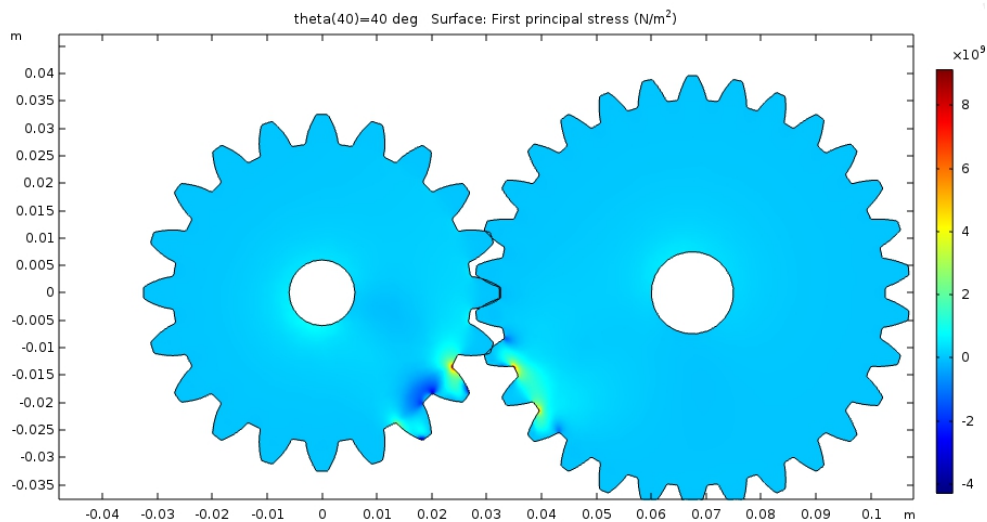


Fig 2: First Surface Principal Stress Model

Furthermore, Figures 3 and 4 present the second and third principal stress as experienced by the spur gear teeth. From Figure 3, the principal stresses were minimal at the gear surfaces and the tooth tip, while it increased at the root fillet and root circle of the gear to about  $2 \times 10^9$  N/m<sup>2</sup>. This could result in severe fatigue damage on the tooth surface as confirmed in the study of Liu et al. [32]. However, Fig 4 demonstrates minimum principal stress. Thus, the issue of rolling contact fatigue, which would have caused pitting and tooth flank fracture would not ensue.

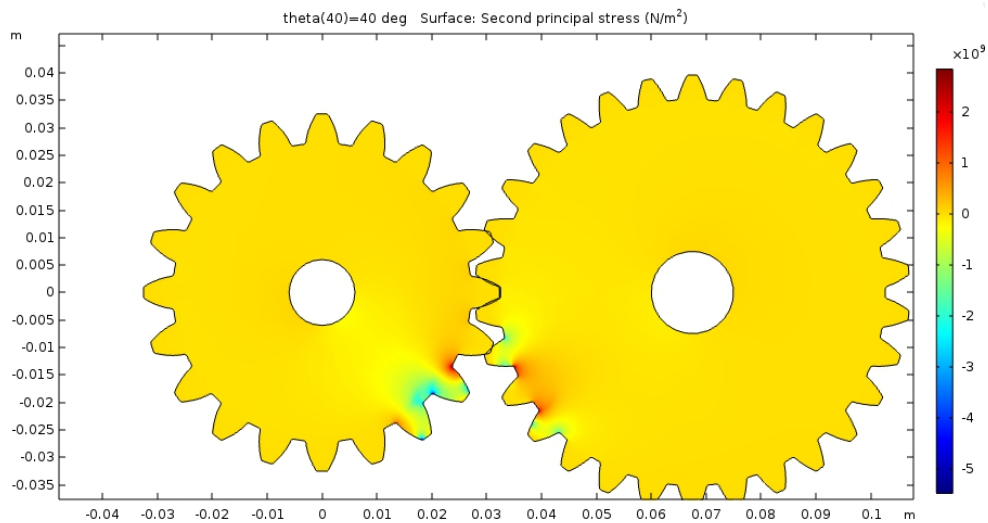


Fig 3: Second Surface Principal Stress Model

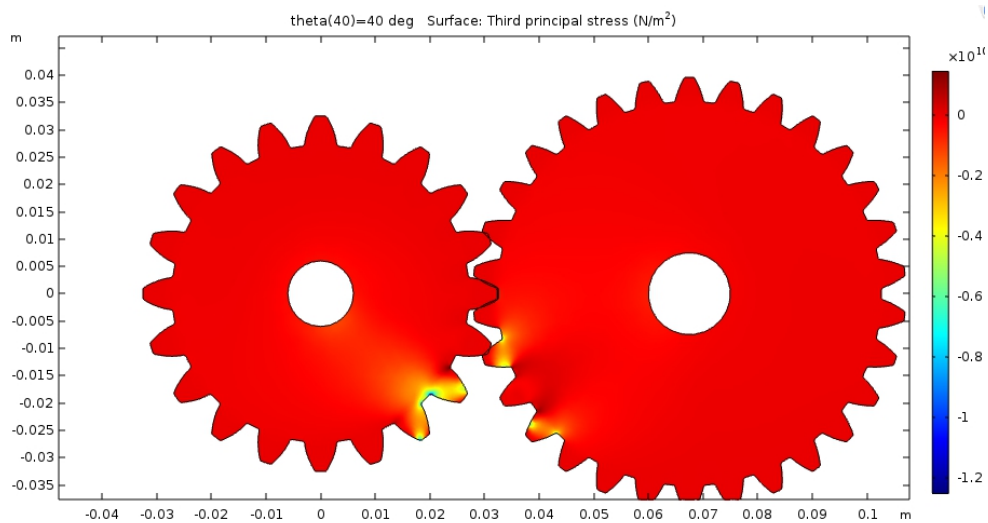


Fig 4: Third Surface Principal Stress Model

Additionally, Figures 5 and 6 present the principal stresses in X and Y-directions. For a pair of spur gear in mesh, two types of motion exist which are sliding and rolling. Both actions could cause a significant increase in stress compared to pure rolling or static conditions. It is on this note that the contact geometry of the meshing is X-axis aligns with the motion direction, while the Y-axis aligns in the axial direction or face width of the gear. Thus, the stresses can be represented in the X and Y component. Maximum principal stress is found within a certain region of the gear geometry which includes; tooth thickness region, gear

surface and probably at the face width and this ranges from 0.2 – 0.8 N/m<sup>2</sup>. This identified regions may be susceptible to wear mechanisms over time.

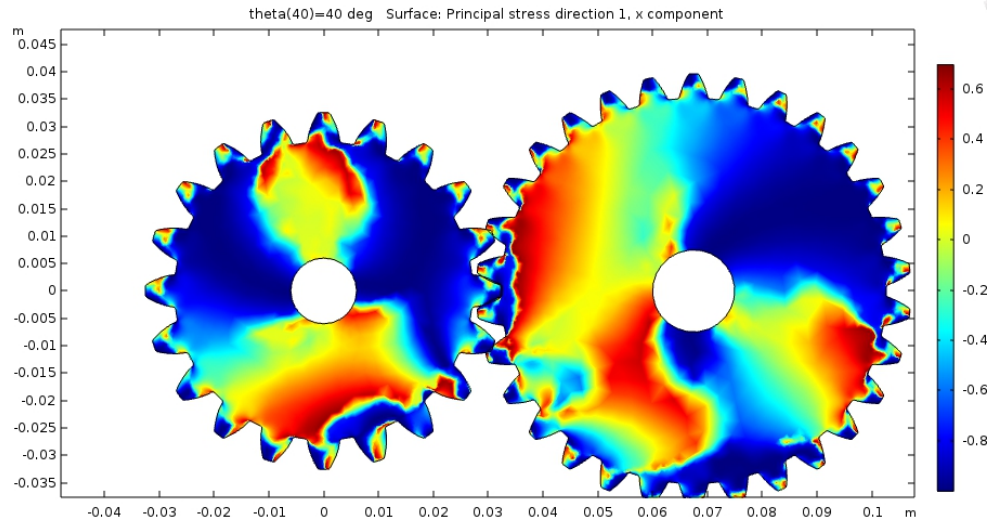


Fig 5: Surface Principal Stress Model in X-direction

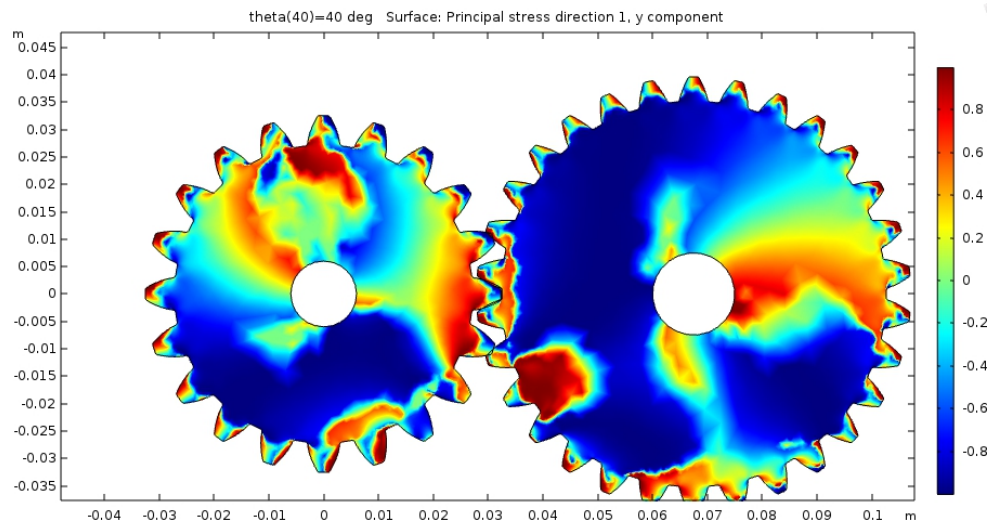


Fig 6: Surface Principal Stress Model in Y-direction

Interestingly, the spur gear in a mesh demonstrates the Von Mises stress effect both at the teeth and at the centre due to the rotational motion of the meshing gear as indicated in Figures 7-8. The minimum Von mises stress occur at the surfaces of the gear, which is seen as the part dominated with blue colour (Figures 7-8). More so, based on the double-tooth and single tooth classification of the contact area in a gear tooth by Qin and Guan [33], it was observed that the maximum Von mises stress spread round the double-tooth (top and root) and the

single-tooth (area near the pitch circle) region of the contacting surface (Figure 7). Thus, it was possible to say that the load distribution under static condition is always felt more at the region near the pitch circle, which usually make this region susceptible to fatigue damage. Additionally, in dynamic analysis of gears, it has also been established that the double-tooth area often experiences incessant failure owing to impact load. Thus, Figure 7 showed maximum Von Mises stress distribution ranging from  $3 - 3.5 \times 10^{-2} \text{ N/m}^2$ .

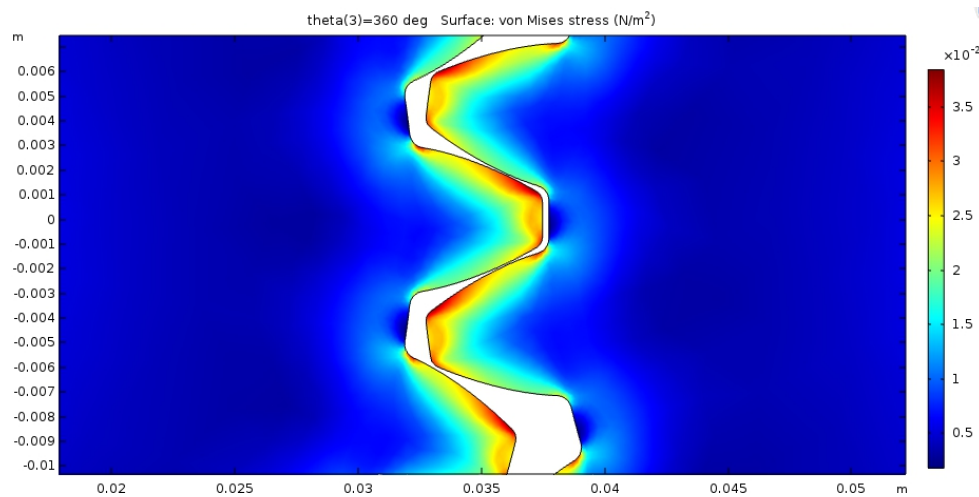


Fig 7: Surface Von Mises stress at the Teeth

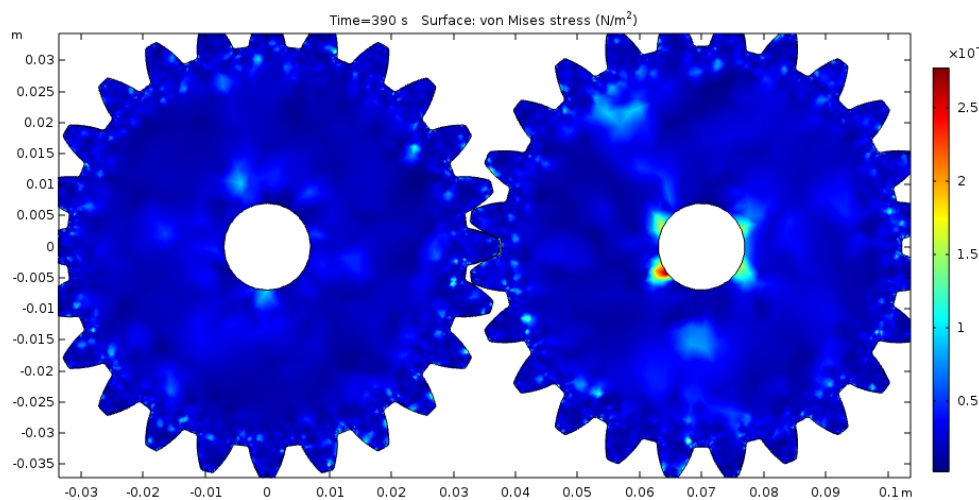


Fig 8: Surface Von Mises stress at the centre

More so, Figure 9 – 11 illustrates the maximum and minimum strain that the gear teeth were subjected to during the simulation. From Figure 9, it was observed that the minimum strain

had a range of  $1 - 2 \times 10^{-3}$ , while the maximum strain ranged from  $2.5 - 3.5 \times 10^{-3}$ . However, Figure 10 showed a minimal strain while in Figure 11, the principal strain was negligible. The variation in the strain values was attributed to the fact that strain rates in structural elements can be rotated just like stress. Thus, the strain at a point on the gear will change when rotated at any angle.

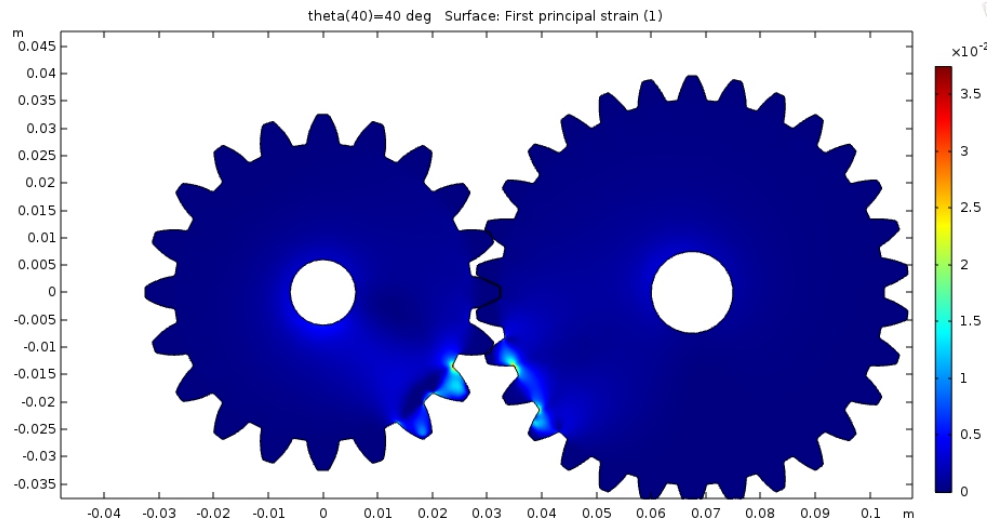


Figure 9: First Principal strain

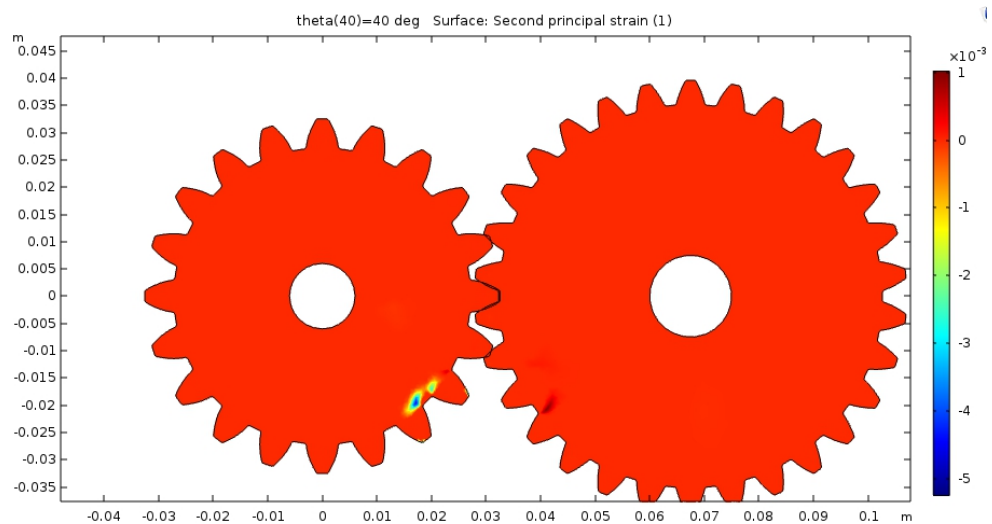


Figure 10: Second Principal strain

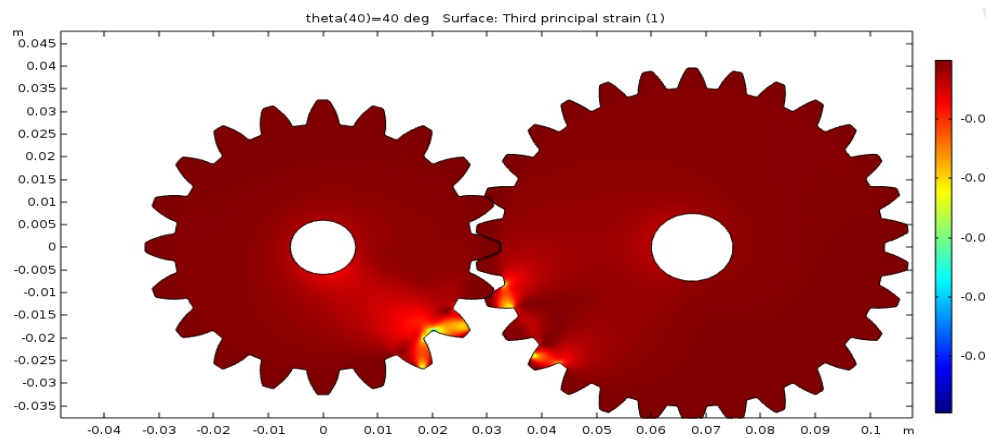


Figure 11: Third Principal strain

Figure 12 represents the volumetric strain which indicates the unit change in volume of the affected area. From the picture, it could be observed that the volumetric strain showed minimum and maximum category. The minimum volumetric change in the gear was evident at the non-contacting surface of the gear, which is showing a zero value. More so, the teeth were observed to experience the maximum volumetric strain of about 0.02. Additionally, in real-life application, increase in tensile strain is expected at the root fillet side of the gear tooth which usually result into non-uniform strain distribution across the tooth thickness, thus making the region susceptible to deformation.

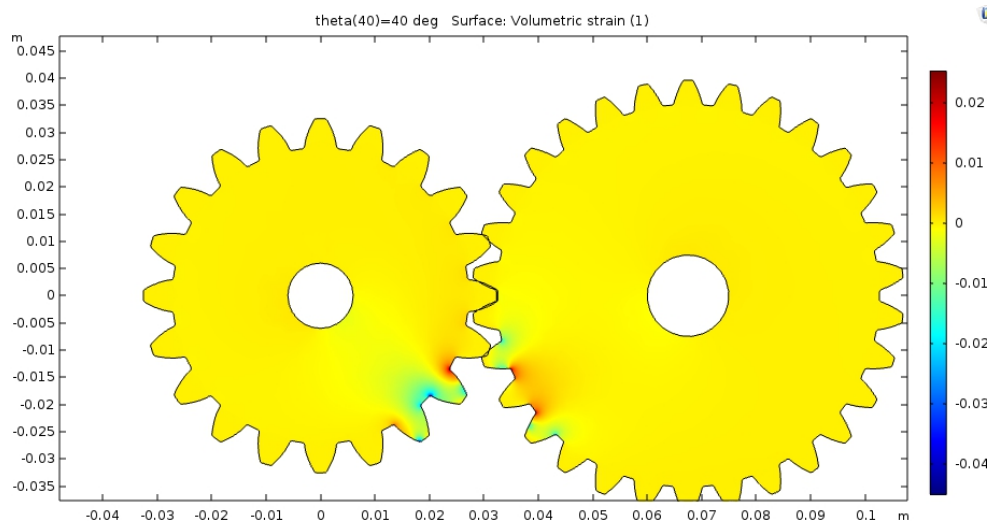


Figure 12: Volumetric strain

Surface displacement at the point of contact and outside the point of contact is often significant in the dynamic analysis of spur gears. However, this has been an area that regularly studies neglect during design. Figure 13 presents the total surface in the pair of meshing gear. Minimum displacement initiates from the centre, which is the shaft position. It

spreads centrally about the middle point of the meshing gears with a minimum value ranging from 0.4 – 1.2 as observed from the colour variation.

Additionally, the maximum displacement dominates the root and tip regions of the gear teeth with a value ranging from 1.2 –  $2.2 \times 10^{-2}$ . More so, this was predominant on the pinion gear. Thus, this prediction method will reduce surface wear of meshing gears.

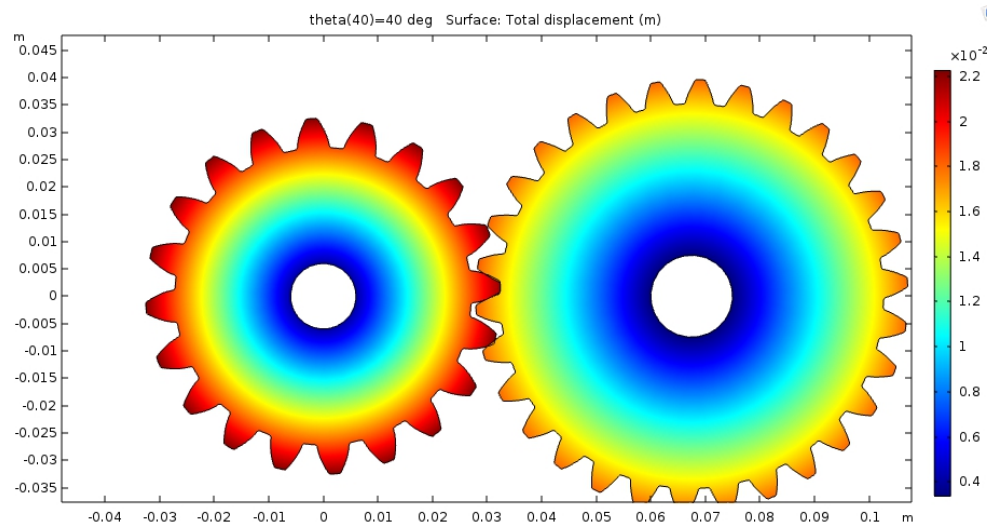


Figure 13: Total displacement

For a pair of gear transmitting power, there is bound to be reaction force and pressure. These forces are classified into tangential (X-component), radial (Y- component) and the axial force, which is known as Z- component. Analysis of these forces is trivial to gear design, especially on the integrated components of gears such as shaft, bearings and key. Based on this, Figures 14 – 16 showed the variation of forces suffered by the pair of meshing gears. Reaction forces occurred at the shaft and the bearings. Thus, the axial forces resulting from the frictional forces at the tooth could give rise to the bearing failure if adequate allowance is not considered during the design. More so, there is a possibility of an increase in the transverse moment due to misalignment, which can be high enough to cause the vibration of the thrust bearings. In addition to these, forces of practical significance are those which result from unbalancing mass. Of course which could be energised by the shaft end deflection, eccentric movement or spacers being out of control during operation at high speed and low torque. Understanding this phenomenon could help in component failure predictions.

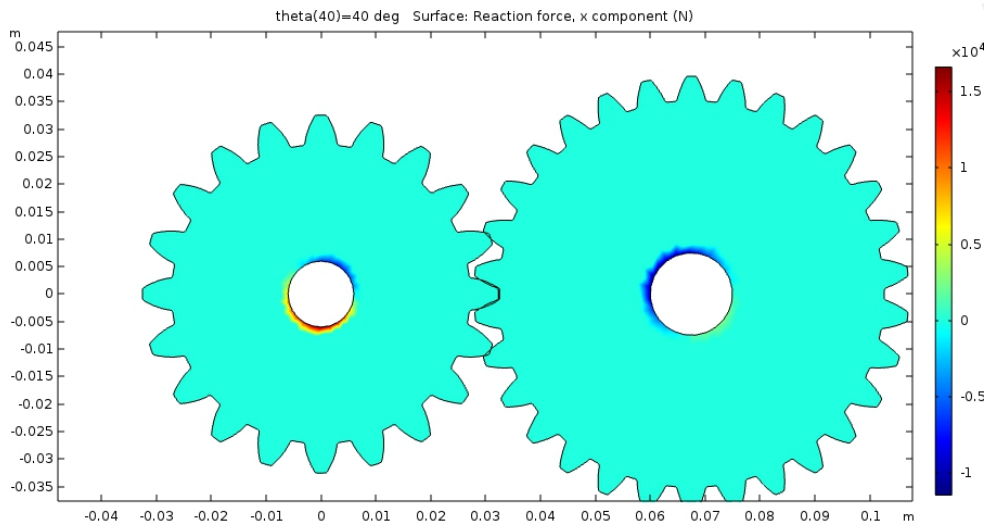


Figure 14: Surface reaction in X-direction

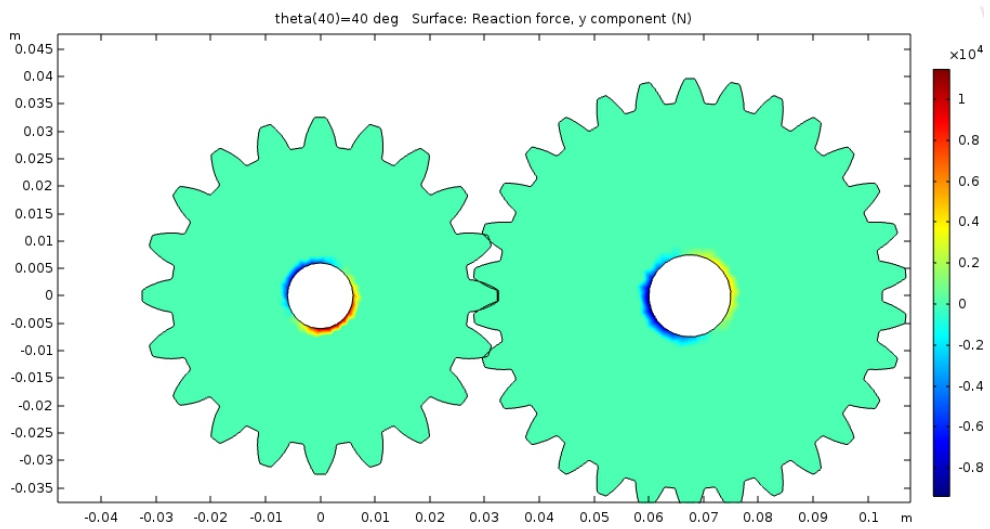


Figure 15: Surface reaction in Y-direction

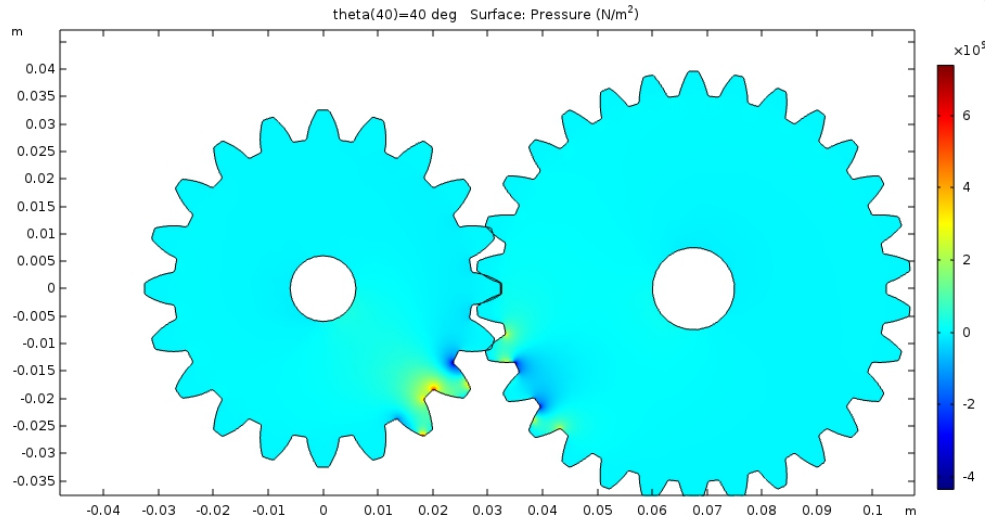


Figure 16: Surface pressure

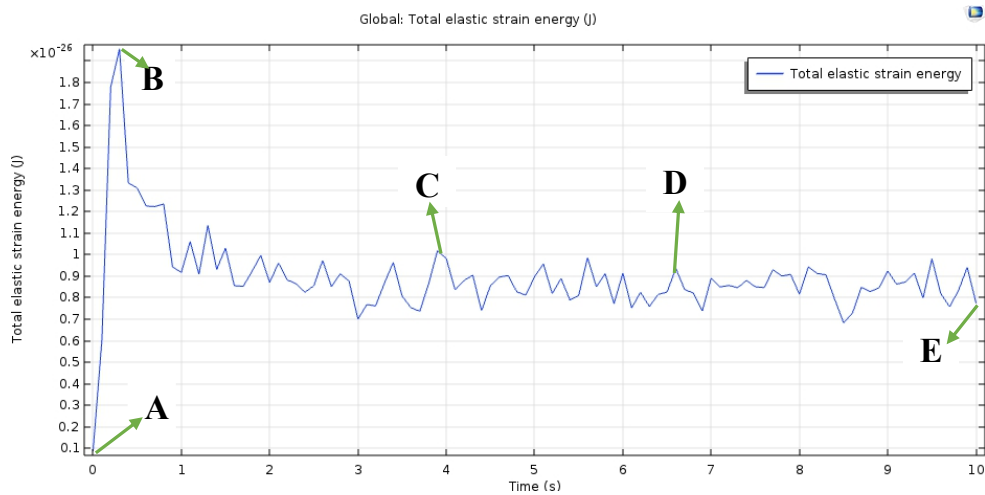


Figure 17: Elastic strain energy

Figure 17 presents the variation of strain energy with time. This is necessary for the proper prediction of gear life expectancy due to the dynamic load distribution while in an application. Point A and E indicate the starting and the ending of a meshing cycle, while points B, C and D show the initial, middle and termination points of a single tooth contact state as established. Based on the evaluated peak strain magnitudes with time, it can be added that the mechanical behaviour of the gear gained the linearly elastic point and eventually decreases into the plastic region. This is important in selecting suitable material during the design.

Figure 18 – 19 presents the variation of the Von Mises stress with time during the cycle. While Figure 18 shows the change in the Von Mises stress during the period, Figure 19

showed the representative plot for the Von Mises stress on the gear teeth. It can be observed that the stress location points are stationary on the teeth. The bottom curves indicate the regions of lower Von Mises stress with the lowest value of about  $0.05 \times 10^{-5} \text{ N/m}^2$ . In comparison, the yellow downward arrows indicate the peak point of maximum Von Mises stress on the teeth with a value of  $0.92 \times 10^{-5} \text{ N/m}^2$ .

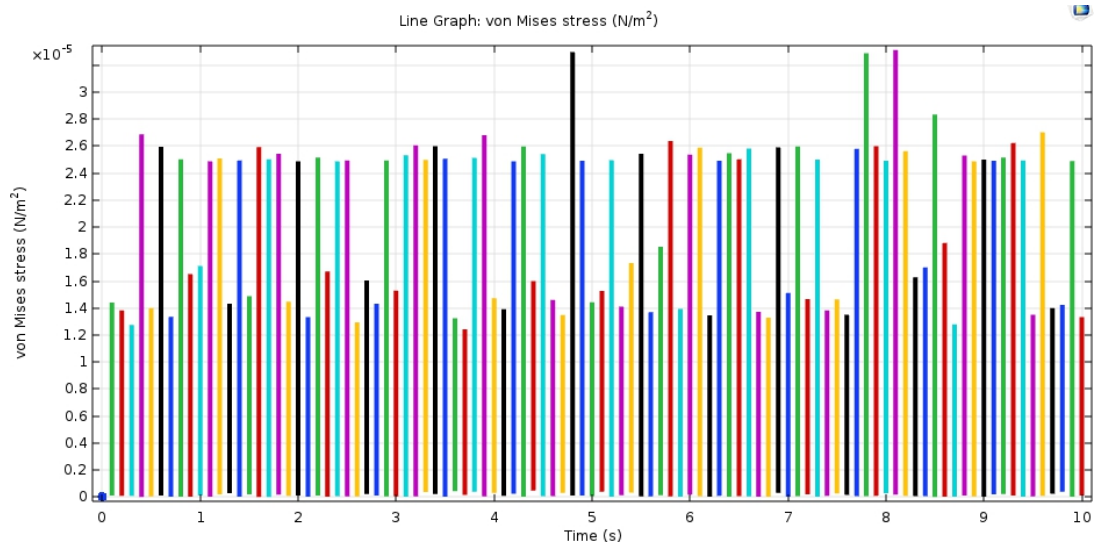


Figure 18: Graphical variation in Von mises stress against Time

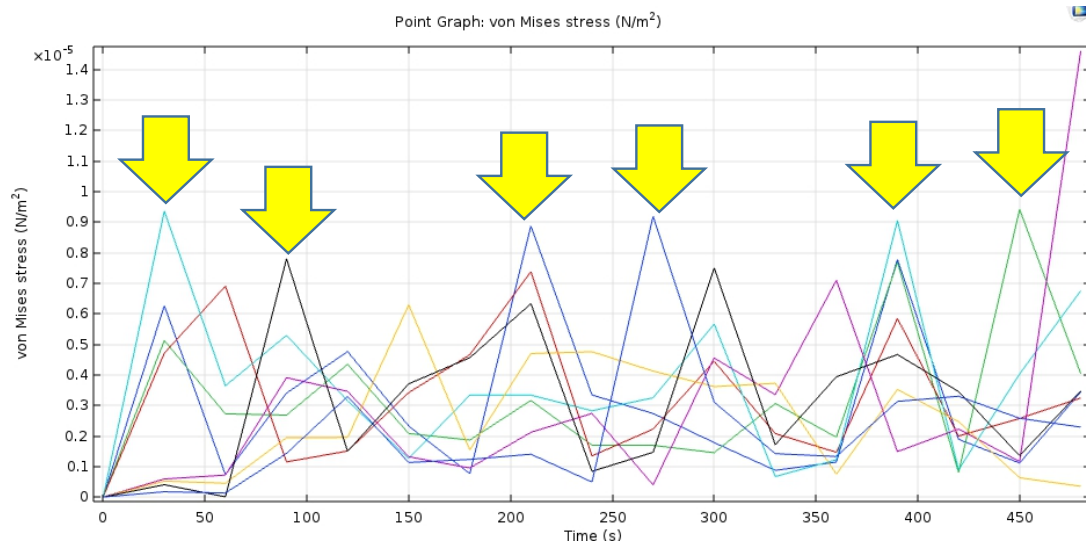


Figure 19: Point graph of Von Mises stress against Time

Lastly, Figure 20 presents the total displacement of the gear against time during the cycle. The displacement of the gear was significant between 50 - 175 seconds. Consequently, this dropped at 200 seconds and assumed a gradual dynamic behaviour. Thus, it could cause system disturbance and subsequent gear failures.

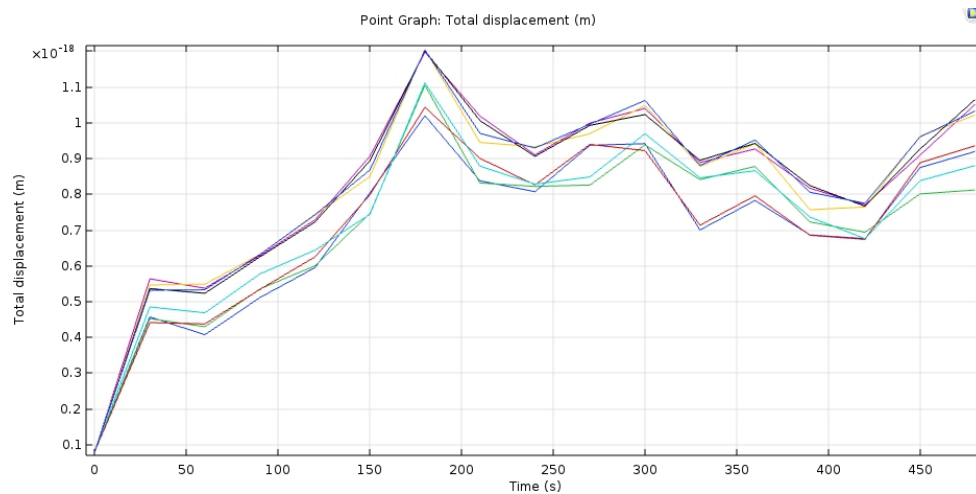


Figure 20: Point graph of Total displacement against Time

## Conclusion

A nonlinear dynamic simulation study of principal stress-strain, volumetric strain and displacement were carried out for a pair of meshing gears. Seven (7) principal stress and three (3) principal strain, including one (1) volumetric strain were established during the simulation. Also, the displacement during the cycle was equally determined. The result demonstrated that the principal stresses were minimal at the gear surfaces and the tooth tip, while it increased at the root fillet and root circle of the gear. More so, the maximum Von Mises stress spread around the double-tooth (top and root) and the single-tooth (area near the pitch circle) region of the contacting surface. Thus, the reason why the load distribution under static condition is always felt more at the region near the pitch circle, which usually make this region susceptible to fatigue damage.

Additionally, in dynamic analysis of gears, it has also been established that the double-tooth region usually experiences incessant failure owing to impact loading. According to the principal strain and the displacement simulation results, the mechanical behaviour of the gear was optimal within the elastic region, which later assumed a plastic region. This result will guide in proper material selection for gear applications. Additionally, the apparent rise at the initial stage during the cycle could cause system disturbance as well as system failures.

## Acknowledgement

The authors appreciate the management of Covenant University for the partial contribution to this study

## Reference

- [1] Zhuang, W., Han, X., Hua, L., Xu, M., & Chen, M. (2019). FE prediction method for tooth variation in hot forging of spur bevel gears. *Journal of Manufacturing Processes*, 38, 244-255.

- [2] Vaghela, P., & Prajapati, J. (2020). Integrated Symmetric and Asymmetric Involute Spur Gear Modelling and Manufacturing. *Materials Today: Proceedings*, 22, 1911-1920.
- [3] Thirumurugan, R., & Gnanasekar, N. (2020). Influence of finite element model, Load-sharing and load distribution on crack propagation path in spur gear drive. *Engineering Failure Analysis*, 104383.
- [4] Salawu, E. Y., Ajayi, O. O., & Inegbenebor, A. O. (2019). Forensic Investigation of a Failed Intermediate Starwheel Spur Gear Tooth in a Filler Machine. *Procedia Manufacturing*, 35, 97-102.
- [5] Patil, V., Chouhan, V., & Pandya, Y. (2019). Geometrical complexity and crack trajectory based fatigue life prediction for a spur gear having tooth root crack. *Engineering Failure Analysis*, 105, 444-465.
- [6] Pleguezuelos, M., Sánchez, M. B., & Pedrero, J. I. (2020). Control of transmission error of high contact ratio spur gears with symmetric profile modifications. *Mechanism and Machine Theory*, 149, 103839.
- [7] Xu, X., Lai, J., Lohmann, C., Tenberge, P., Weibring, M., & Dong, P. (2019). A model to predict initiation and propagation of micro-pitting on tooth flanks of spur gears. *International Journal of Fatigue*, 122, 106-115.
- [8] Zhou, R., Zhao, N., Li, W., Li, R., Guo, G., & Guo, H. (2019). A grinding method of face gear mating with a conical spur involute pinion. *Mechanism and Machine Theory*, 141, 226-244.
- [9] Xu, X., Lai, J., Lohmann, C., Tenberge, P., Weibring, M., & Dong, P. (2019). A model to predict initiation and propagation of micro-pitting on tooth flanks of spur gears. *International Journal of Fatigue*, 122, 106-115.
- [10] Salawu, E. Y., Ajayi, O. O., Inegbenebor, A., Akinlabi, S., Akinlabi, E., & Ishola, F. Influence of Von Mises Stress on the Deformation behaviour of a Pinion Spur Gear under Cyclic Loading in a Bottling Machine: An Approach for predicting surface Fatigue failure in Gears. *International Journal of Engineering Research and Technology*. 12, 2207-2211.
- [11] Salawu, E. Y., Ajayi, O. O., Inegbenebor, A. O., & Afolalu, S. A. (2019). Constitutive Model to Analyse the effect of Variation in Temperature Distribution on the Rate of Heat Transfer around a Spur Gear Tooth. *Procedia Manufacturing*, 35, 236-241.
- [12] Zhuang, W., Hua, L., & Han, X. (2018). Influences of key forging parameters on gear-tooth deviation of cold forged spur bevel gear. *Procedia Manufacturing*, 15, 504-510.
- [13] Liu, X., Huang, H., & Xiang, J. (2020). A personalised diagnosis method to detect faults in gears using numerical simulation and extreme learning machine. *Knowledge-Based Systems*, 105653.
- [14] Zhiying, C., & Pengfei, J. (2020). Study on wear in spur gears based on an improved load distribution model considering the effects of corner contact. *Engineering Failure Analysis*, 104605.
- [15] Ouyang, T., Huang, H., Zhou, X., Pan, M., Chen, N., & Lv, D. (2018). A finite line contact tribo-dynamic model of a spur gear pair. *Tribology International*, 119, 753-765.

- [16] Yi, Y., Huang, K., Xiong, Y., & Sang, M. (2019). Nonlinear dynamic modelling and analysis for a spur gear system with time-varying pressure angle and gear backlash. *Mechanical Systems and Signal Processing*, 132, 18-34.
- [17] Černe, B., Petkovšek, M., Duhovnik, J., & Tavčar, J. (2020). Thermo-mechanical modeling of polymer spur gears with experimental validation using high-speed infrared thermography. *Mechanism and Machine Theory*, 146, 103734.
- [18] Chen, Z., Zhou, Z., Zhai, W., & Wang, K. (2020). Improved analytical calculation model of spur gear mesh excitations with tooth profile deviations. *Mechanism and Machine Theory*, 149, 103838.
- [19] Tang, X., Zou, L., Yang, W., Huang, Y., & Wang, H. (2018). Novel mathematical modelling methods of comprehensive mesh stiffness for spur and helical gears. *Applied Mathematical Modelling*, 64, 524-540.
- [20] Černe, B., Duhovnik, J., & Tavčar, J. (2019). Semi-analytical flash temperature model for thermoplastic polymer spur gears with consideration of linear thermo-mechanical material characteristics. *Journal of Computational Design and Engineering*, 6(4), 617-628.
- [21] Sánchez, M. B., Pleguezuelos, M., & Pedrero, J. I. (2019). Strength model for bending and pitting calculations of internal spur gears. *Mechanism and Machine Theory*, 133, 691-705.
- [22] Shi, J. F., Gou, X. F., & Zhu, L. Y. (2019). Modeling and analysis of a spur gear pair considering multi-state mesh with time-varying parameters and backlash. *Mechanism and Machine Theory*, 134, 582-603.
- [23] Cirelli, M., Valentini, P. P., & Pennestri, E. (2019). A study of the nonlinear dynamic response of spur gear using a multibody contact based model with flexible teeth. *Journal of Sound and Vibration*, 445, 148-167.
- [24] Wen, Q., Du, Q., & Zhai, X. (2018). A new analytical model to calculate the maximum tooth root stress and critical section location of spur gear. *Mechanism and Machine Theory*, 128, 275-286.
- [25] Chen, T., Wang, Y., & Chen, Z. (2019). A novel distribution model of multiple teeth pits for evaluating time-varying mesh stiffness of external spur gears. *Mechanical Systems and Signal Processing*, 129, 479-501.
- [26] Osman, T., & Velex, P. (2012). A model for the simulation of the interactions between dynamic tooth loads and contact fatigue in spur gears. *Tribology International*, 46(1), 84-96.
- [27] Osman, T., & Velex, P. (2010). Static and dynamic simulations of mild abrasive wear in wide-faced solid spur and helical gears. *Mechanism and Machine Theory*, 45(6), 911-924.
- [28] Bobach, L., Beilicke, R., Bartel, D., & Deters, L. (2012). Thermal elastohydrodynamic simulation of involute spur gears incorporating mixed friction. *Tribology International*, 48, 191-206.
- [29] Litvin, F. L., Lian, Q., & Kapelevich, A. L. (2000). Asymmetric modified spur gear drives: reduction of noise, localisation of contact, simulation of meshing and stress analysis. *Computer methods in applied mechanics and engineering*, 188(1-3), 363-390.

- [30] Zhang, Z., & Xie, J. (2006). A numerical simulation of super-plastic die forging process for Zr-based bulk metallic glass spur gear. *Materials Science and Engineering: A*, 433(1-2), 323-328.
- [31] Patil, S. S., Karuppanan, S., & Atanasovska, I. (2016). Experimental measurement of strain and stress state at the contacting helical gear pairs. *Measurement*, 82, 313-322.
- [32] Liu, H., Wang, W., Zhu, C., Jiang, C., Wu, W., & Parker, R. G. (2019). A microstructure sensitive contact fatigue model of a carburised gear. *Wear*, 436, 203035.
- [33] Qin, W. J., & Guan, C. Y. (2014). An investigation of contact stresses and crack initiation in spur gears based on finite element dynamics analysis. *International Journal of Mechanical Sciences*, 83, 96-103.